

FERMILAB-CONF-05-432-E

# Results from the Cryogenic Dark Matter Search at Soudan Underground Laboratory<sup>1</sup>

Jonghee Yoo<sup>2</sup>  
for CDMS Collaboration

*Fermi National Accelerator Laboratory, Batavia, IL 60510*

**Abstract.** We present results from the Cryogenic Dark Matter Search at Soudan Underground Laboratory for two-tower arrays of detector. Twelve detectors were operated from March 25 to August 8, 2004, or 74.5 detector live days. Within expected background, no statistically significant indication of a WIMP signal was observed. Based on this null observation and combined with our previous results, we exclude a spin-averaged WIMP-nucleon interaction cross section above  $1.6 \times 10^{-43} \text{ cm}^2$  for Ge detectors, and  $3 \times 10^{-42} \text{ cm}^2$  for Si detectors, for a WIMP mass  $60 \text{ GeV}/c^2$  with 90% C.L. This result constrains parameter space of minimal supersymmetric standard models (MSSM) and starts to reach the parameter space of a constrained model (CMSSM).

**Keywords:** Dark Matter, WIMPs, CDMS

**PACS:** 95.35.+d, 95.30.Cq, 85.25.Oj, 29.40.Wk, 14.80.Ly

## INTRODUCTION

It is mysterious that 95% of the Universe cannot be explained by ordinary matter components. However, there is increasing consensus among cosmologists that 70% of the Universe consists of an unknown energy component and 25% of the Universe consists of an unknown matter component. The observations of rotational curves of galaxies, cosmic microwave background anisotropies, large scale structure, galaxy clusters, gravitational lensing, and most recently WMAP and SDSS experiments provide strong evidence that a nonluminous, nonbaryonic component, so called Dark Matter, may constitute most of the matter in the Universe [1].

There is no lack of particle candidates that could explain the Dark Matter component. Among those particles, weakly interacting massive particles (WIMPs) are currently the most interesting for two reasons. First, WIMPs (neutralinos in most cases) naturally appear in most supersymmetric scenarios, and it is relatively simple to construct a stable particle by requiring certain symmetries such as R-parity. Second, the expected interaction cross-section of WIMPs with normal matter and its mass range are the most experimentally accessible among Dark Matter candidates [2][3].

Although there are a lot of possible scenarios and no standard agreement on the distribution of Dark Matter in the Universe, it is usually assumed to form a roughly isothermal spherical halo around our galaxy with Maxwell-Boltzmann velocity distribution at a mean of  $\sim 230 \text{ km/sec}$ , and escape velocity from the galactic halo of  $\sim 650 \text{ km/sec}$  [4].

The mass range of  $50 - 500 \text{ GeV}$  is particularly interesting for direct detection of WIMP particles. In this mass range, together with the velocity distributions discussed above, the WIMP-nucleon scattering would result in an energy deposition in the detector of a few to tens of keV [5].

The Cryogenic Dark Matter Search (CDMS) experiment is designed to detect a WIMP signal through nuclear recoil by elastic scattering. The detector is capable of reading out both the phonon-energy and the ionization-energy of an interaction in Ge or Si crystals. The CDMS-I experiment was carried out in the Stanford Underground Facility and the performance of detectors had been successfully demonstrated there. In order to reduce cosmic-ray induced backgrounds, the detector was installed in Soudan Underground Laboratory. This is called the CDMS-II experiment. There have been two separate phases of CDMS-II experiment. The first phase was a single tower (4 Ge and 2 Si detectors) operation and the second phase was a two-tower (6 Ge and 6 Si detectors) operation. We present here the results of the second phase of the CDMS-II experiment.

<sup>1</sup> The talk was given at the PASCOS-05 conference plenary session, held in May 30 - Jun 4, 2005 Gyeongju, Korea.

<sup>2</sup> yoo@fnal.gov

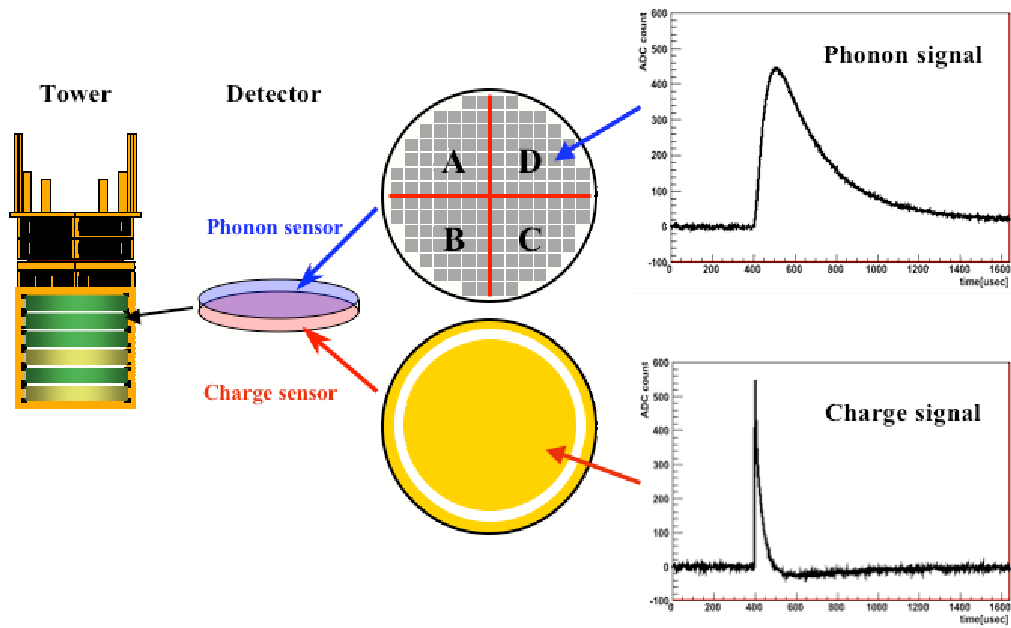


**FIGURE 1.** Schematics of the ZIP detector and its signal. The left most figure shows the detector array. The different shading indicates the different crystals (Ge or Si). The charge (ionization) channel consists of two concentric electrodes. The phonon sensor has four separate channels. An example of the pulse shape in time domain for each channel is shown at right.

## CDMS EXPERIMENT

The idea of CDMS Z(depth)-sensitive Ionization and Phonon detectors (ZIPs) is to discriminate WIMP-nucleus recoil energy by measuring both the ionization and phonon signal from the crystal [6]. The ZIP detector is an ultra-pure Ge (250 g) or Si (100 g) crystal in a cylindrical shape of 1 cm thick and 7.6 cm diameter. A tower consists of a vertically stacked 6 ZIP detector-array. Figure 1 shows a schematic of a ZIP detector array (tower) and examples of signals from each channel. The detectors are cooled by a dilution refrigerator down to 50 mK. This cryogenic configuration prevents background signals from thermal excitations in the crystal. The ionization signal is the interaction that breaks the electron-hole pairs of the semiconductor crystal. The electron and hole pairs are separated by an electric field through the crystal. The ionization signals are then read out by inner and outer electrodes. The inner electrode covers 85% of the ionization side of the detector. The events from the edge area of the detector have suppressed phonon energy collections and the outer electrode is used to discriminate those edge-events. The phonon signals that are produced by the vibration of crystal lattice are read out by a total of 4144 Quasiparticle-assisted Electrothermal-feedback Transition-edge sensors (QETs) on each detector. Each QET consists of a 1  $\mu\text{m}$  wide strip of tungsten connected to 8 superconducting aluminum collection fins

which cover the phonon sensor side of the crystal. The tungsten strips, on Transition-Edge-Sensors (TESs), are voltage biased, with the current through them monitored by a high-bandwidth SQUID array.

When an interaction occurs in the crystal, a huge amount of phonons are produced. Most of the phonons that reach the surface of a phonon sensor area can scatter into the aluminum fins. The athermal phonons, energetic enough (above 340  $\mu\text{eV}$ ) to break Cooper pairs in a superconducting state of aluminum fins, produce quasiparticles. The quasiparticles enter into the TESs. The interaction between the quasiparticles and conduction electrons in the TESs increases the temperature of the system and hence increases the resistance of the tungsten. The increase of resistance decreases the current supplied by the voltage bias. The reduction of Joule heating from the voltage bias lowers the temperature of the tungsten. This strong electro-thermal-feed-back guarantees that the power deposited into the TES is exactly compensated for by a reduction in Joule heating. Then the energy deposited can be measured by reading out the change of current.

In order to understand the detector response, detector calibrations have been occasionally carried out during the normal data-taking period. A  $^{133}\text{Ba}$  gamma-ray source is used to calibrate energy scale and to characterize detector response to electron recoils. A  $^{252}\text{Cf}$  neutron source is used to characterize the detector response of

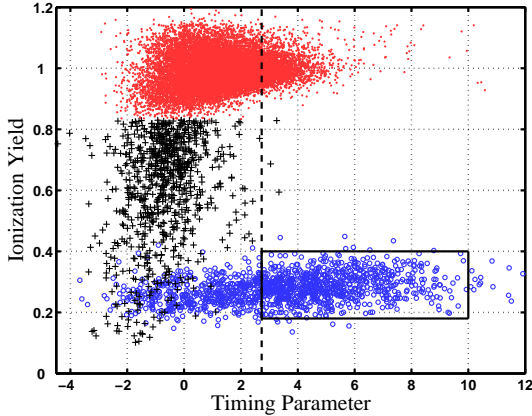


**FIGURE 2.** Ionization yield versus summed timing parameter for calibration data in a Ge detector with the recoil energy range 10–100 keV. The ionization yield shows clear separation between bulk-electron recoil events (dots and yield near 1.0; from  $^{133}\text{Ba}$  calibration source) from nuclear recoil events (circles and yield near 0.3; from  $^{252}\text{Cf}$  calibration source). The surface-electron recoil events (crosses) from  $^{133}\text{Ba}$  show wide distribution along the ionization yield and non-negligible amount of events are leaked into nuclear recoil area. The timing parameter has discrimination power of those electron leak events. The vertical dashed line shows the minimum allowed timing parameter for WIMP candidate event. The squared area is an allowed region of nuclear recoil.

nuclear recoils produced by neutrons. Results of Monte Carlo simulations of  $^{133}\text{Ba}$  and  $^{252}\text{Cf}$  calibration show good agreement with data.

## BACKGROUNDS

In order to detect a non-Standard Model particle, all Standard Model particles that can be seen by the detector are background sources. Once all backgrounds are identified or removed, the remaining events that cannot be understood within the Standard Model scheme are candidates of new particles. Therefore the major efforts of any Dark Matter search experiment are in fact all about backgrounds.

The ionization signals produced by a nuclear recoil, which WIMPs may cause, are suppressed compared to the ionization signals from electron recoils, while phonon signals are the same. Therefore the ratio between ionization and phonon (recoil) energy, termed ionization yield, provides strong discrimination power of background events such as gammas. However, the events within  $35\ \mu\text{m}$  of the detector surface suffer ionization yield suppression. Therefore, some of those surface events could be misidentified as nuclear recoils. The timing information, such as start time and rise time of the phonon pulse, helps to reject 97% of these surface

events while keeping 70% of true nuclear recoils. Figure 2 shows ionization yield versus a summed timing parameter for calibration data of  $^{133}\text{Ba}$  and  $^{252}\text{Cf}$  sources. The ionization yield shows clear separation between bulk-electron recoil events from nuclear recoil events. The surface-electron recoil events can be excluded by setting a timing parameter cut. The squared area in the figure is defined as a WIMP signal region before looking at the WIMP search data sample.

A neutron recoil event cannot be discriminated from a WIMP-nuclear recoil event by looking at only a single detector signature. Since the WIMP is supposed to interact weakly ( $<10^{-42}\text{cm}^2$ ), the mean free path in Ge is order of  $10^{10}\text{m}$ . Therefore WIMPs will scatter a single time while neutrons can multiple scatter in the detector array. By choosing only single scatter events, the neutron events can be further reduced. Moreover the interaction rate of WIMPs in nuclei is expected to be proportional to mass-square ( $\propto A^2$ ) of the target nuclei. Accordingly the WIMP interaction rate in  $^{73}\text{Ge}$  is  $\sim 6$  times larger than  $^{28}\text{Si}$  while neutron interaction rates are similar for both crystals. Therefore once we observe the number of WIMP candidate signals in several detectors, comparison of event rates between Ge and Si detectors will provide statistically strong discrimination power between neutrons and WIMPs.

The CDMS-I experiment had been carried out at the Stanford Underground Facility (SUF), California, USA at a depth of 10.6 m (17 meters water equivalent). Photon and neutron backgrounds were reduced by layers of shielding materials such as lead and polyethylene respectively. Scintillator panels surrounding the passive shielding composed the active moun veto. The expected cosmic-ray muon background rate in this shallow site was  $50\ \mu\text{ons sec}^{-1}\text{m}^{-2}$ . Neutrons, the most serious background source at SUF, gave a rate of  $\sim 1\ \text{event kg}^{-1}\text{day}^{-1}$ . A single tower, total 6 detectors (4 Ge + 2 Si), was operated from December 2001 to April 2003 for a total of 65.8 detector live days and 28.3 kg-day of net exposure. Twenty nuclear recoil events were observed from the WIMP search data sample and those agreed with the expected neutron background rate[12].

The CDMS-II experiment, a single tower operation with the identical detector configuration at SUF, was carried out in the Soudan Underground Laboratory, Minnesota, USA, at a depth of 780 m from the surface (2090 meters water equivalent). The cosmic muon rate was reduced down to  $0.25\ \mu\text{ons min}^{-1}\text{m}^{-2}$ . Neutron background rate is estimated to be  $1\ \text{event kg}^{-1}\text{year}^{-1}$ . The rate of unvetoes neutron induced recoils is  $3 \times 10^{-4}\ \text{kg}^{-1}\text{day}^{-1}$  and is estimated by Monte Carlo simulation. This experimental background configuration is sufficient enough to carry out 1000 kg-day of detector exposure to the WIMP search without neutron background contamination. The detectors were operated from Octo-

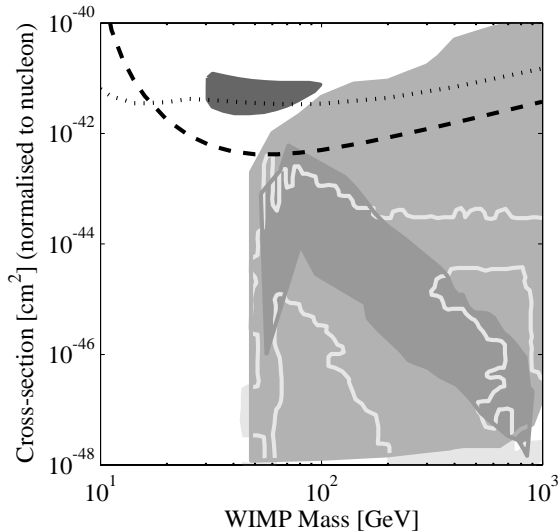


**FIGURE 3.** WIMP-nucleon cross section upper limits (90% C.L.) versus WIMP mass. The experimental upper limits of WIMP-nucleon cross section is compared with some theoretical models (the large gray area is from Kim et al.[7], dark gray area is CMSSM region from Ellis et al.[8] and light gray line is from Baltz et al.[9]) together with allowed region by DAMA[10] experiment (filled black area). Figure conventions for theoretical and DAMA regions are all the same for successive figures in this proceeding. The dotted curve uses results from shallow site (SUF). The dashed curve uses results from deep site (Soudan). The Soudan result gives factor 10 improvement of WIMP search sensitivity with almost identical detector configuration. This and successive limit-curve figures are produced by using [11].

ber 2003 to January 2004 for a total of 52.6 detector live days and 19.4 kg-day of net exposure. In contrast to the SUF background configuration, electron-recoil events now become the dominant source of background in the Soudan Underground Laboratory. The number of electron-recoil events expected to be misidentified as nuclear recoils in the WIMP-search data were estimated total  $0.7 \pm 0.3$  (systematic errors are factored) in Ge detectors. The analysis results found one nuclear-recoil candidate event at 64 keV, consistent with the expected background event[13][14]. The above two separate operations of CDMS detectors in identical condition except different depth clearly demonstrate that the neutron backgrounds produced from cosmic-rays are substantially reduced by going deeper site. Figure 3 shows the limit of WIMP-nucleus cross section in recoil energy based on null observation of WIMP signal in SUF (dotted curve) and Soudan (dashed curve). The result demonstrates a factor of 10 improvement of WIMP-nucleus interaction sensitivity in Soudan compared with that of SUF.

The second phase of the CDMS-II experiment, two towers operation, is carried out with the same configu-

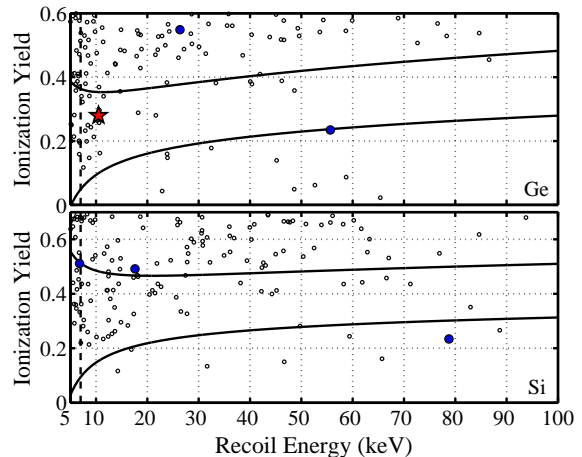


**FIGURE 4.** Ionization yield versus recoil energy events for Ge (upper figure) and Si (lower figure) detectors before (small circles, solid dots and star mark) and after (solid dots and star mark) surface electron recoil rejection cut (timing parameter cut). The 7 keV energy threshold is shown in vertical dashed line in each figure. The ionization yield between curved lines in each figure is WIMP signal region. One candidate event is found in WIMP search signal band in Ge detector with recoil energy of 10.5 keV (shown in star mark in upper figure).

ration of the first phase except 6 more detectors. The operation period was from March 25 to August 8, 2004 for a total of 74.5 detector live days and 34 kg-day (13 kg-day) net exposure for Ge (Si) detectors.

## DATA ANALYSIS

We exclude data sets with known problems such as events triggered by noise burst, non-operational channels and failure of off-line diagnostics. For recoil energies above  $\sim 10$  keV, events due to background photons are rejected with  $> 99.99\%$  efficiency. Electromagnetic events very near the detector surface can mimic nuclear recoils because of reduced charge collection. These surface events, however, are rejected with  $> 96\%$  efficiency by using additional phonon pulse shape information.

To calculate a signal band area of electron-recoil events in ionization yield (=ionization energy / recoil energy) versus recoil energy parameter space, we first carry out a Gaussian fit to the distributions of ionization yield for both  $^{133}\text{Ba}$  calibration and  $^{252}\text{Cf}$  calibrations in several recoil energy bins. The estimated means and standard deviations are then fitted versus recoil energy. The band-width of the electron-recoil and nuclear-recoil are taken to be  $\pm 2\sigma$ . The muon events that have coincident hits in the veto counter in the predefined time window are removed. Then we choose single scatter events, which have a signal only in one out of the 12 detectors.

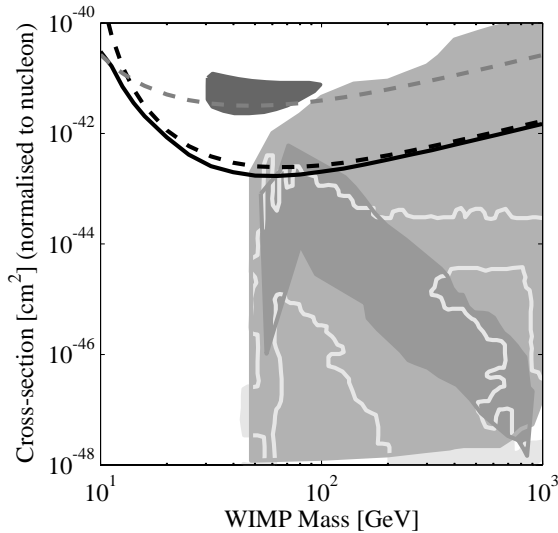


**FIGURE 5.** New result of WIMP-nucleon cross section upper limits (90% C.L.) versus WIMP mass. The gray-dashed line on the top is results from Si detectors. The black-dashed line in the middle is result from Ge detectors. The black-solid line is combined limit of all previous and new results.

Events with low ionization yield in the  $^{133}\text{Ba}$  calibration data, which presumably come from surface electron recoils, were used to develop rejection cut criteria. Phonon pulses from surface recoils are more prompt than those from recoils in the detector bulk. Two timing quantities in the quadrant with the largest phonon signal are useful; the time delay of the phonon signal relative to the fast ionization signal and the phonon pulse rise time. The sum of delay and rise time forms a timing parameter, where energy corrections to the delay and rise time are applied to achieve energy-independence (see figure 2).

The surface event backgrounds at WIMP search signal region (nuclear recoil band) are estimated before unmasking the WIMP search data using multiple-detector events that pass timing cuts. The expected background rate is based on the passing fraction between 10–100 keV in the WIMP-search data, assumed to be similar to the single-scatter event background. The number of surface background events expected to pass the timing cuts are  $0.4 \pm 0.2(\text{stat}) \pm 0.2(\text{syst})$  between 10–100 keV in Ge detectors and  $1.2 \pm 0.6(\text{stat}) \pm 0.2(\text{syst})$  between 7–100 keV in Si detectors. From simulations, the expected background from unvetoes nuclear recoils due to impinging cosmogenic neutrons is 0.06 events in Ge and 0.05 events in Si so it is negligible compared with surface electron background contribution.

After unmasking the WIMP search data, one candidate with 10.5 keV recoil energy was found to pass all cuts. Figure 4 shows the unmasked WIMP search data in

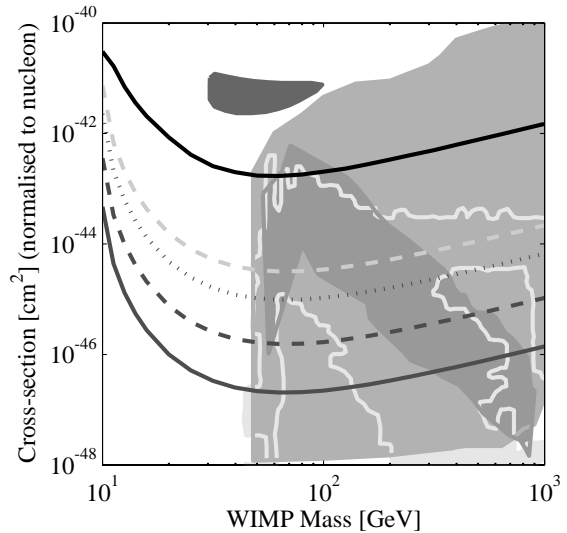


**FIGURE 6.** WIMP search sensitivity (projected). The black-solid line at the top is the new best limit (CDMS-II combined limit). The gray-dashed line at the second is the projected limit for third phase (five tower) of CDMS-II. The consecutive dotted, dashed and solid lines are projected limit for SuperCDMS phase A, B and C respectively.

ionization yield versus recoil energy for both Ge (upper figure) and Si (lower figure). It turned out that the candidate occurred in a detector during an interval of time when that detector suffered inefficient ionization collection. Even though we count the event as a WIMP candidate, it is still consistent with the rate of expected background.

Figure 5 shows the upper limits on WIMP-nucleon cross sections calculated from the results of two-tower operations using the assumption of spherical distributions of the galactic halo. We exclude spin-averaged WIMP-nucleon interaction cross section above  $1.6 \times 10^{-43} \text{ cm}^2$  from Ge detectors and  $3 \times 10^{-42} \text{ cm}^2$  from Si detectors, for WIMP mass  $60 \text{ GeV}/c^2$  with 90% C.L. This result constrains parameter space of minimal supersymmetric standard models (MSSM) and starts to reach a parameter space of a constrained model (CMSSM) [15].

## SHORT AND LONG TERM PLANS

The CDMS experiment demonstrated that the ZIP detector is currently the most proven technique to carry out a Dark Matter search without background. The excellent background rejection power provides the experiment with a sensitivity directly proportional to the mass of the detector and exposure time ( $MT$ ) rather than the square root of them ( $\sqrt{MT}$ ). Increasing the total mass of the de-

tectors is the most efficient way to test smaller WIMP-nucleon cross sections.

The next phase of the CDMS-II experiment is the operation of five tower (19 Ge and 11 Si, total 5.85 kg) detector arrays which is currently under commissioning and planned to operate until the end of year 2007. The five tower operation will provide another factor ten in sensitivity of WIMP-nucleon cross section.

Long term plans of the CDMS the project is implementing a super array (total a ton scale) of ZIP detectors in a deeper site than Soudan, such as SNOLab. The project is named SuperCDMS[16]. In order to maximize discovery potential, the SuperCDMS experiment plans to operate three separate phases. Each phase has a different mass scale; 25 kg-phase-A (2011), 150 kg-phase-B (2014) and 1,000 kg-phase-C (2018). Figure 6 shows projected WIMP search potential for each phase of detector operation. The SuperCDMS experiment can scan most of the region of WIMP-nucleon cross-section and mass parameter spaces. An exciting period is around the corner.

## ACKNOWLEDGMENTS

This work is supported by the National Science Foundation under Grant No. PHY-9722414, by the Department of Energy under contracts DE-AC03-76SF00098, DE-FG03-90ER40569, DE-FG03-91ER40618, DE-FG02-94ER40823, and by Fermilab, operated by the Universities Research Association, Inc., under Contract No. DE-AC02-76CH03000 with the Department of Energy. The ZIP detectors were fabricated in the Stanford Nanofabrication Facility operated under NSF.

## REFERENCES

1. D. N. Spergel *et al.*, (WMAP Collab.), *Astrophys. J. Suppl.* **148**, 175 (2003); M. Tegmark *et al.*, (SDSS Collab.), *Phys. Rev. D* **69**, 103501 (2004).
2. G. Steigman and M.S. Turner, *Nucl. Phys.* **B253**, 375 (1985).
3. G. Jungman, M. Kamionkowski, and K. Griest, *Phys. Rep.* **267**, 195 (1996); G. Bertone, D. Hooper, and J. Silk, *Phys. Rep.* **405**, 279 (2005).
4. P. Salucci and A. Borriello, *Lect. Notes Phys.* **616**, 66 (2003); T. Broadhurst *et al.*, *Astrophys. J.* **621**, 53 (2005).
5. J. D. Lewin and P. F. Smith, *Astropart. Phys.* **6**, 87, (1996).
6. K.D. Irwin *et al.*, *Rev. Sci. Instr.* **66**, 5322 (1995); T. Saab *et al.*, *AIP Proc.* **605**, 497, (2002).
7. Y. G. Kim *et al.*, *JHEP* **12**, 034 (2002).
8. J. Ellis *et al.*, *Phys. Rev. D* **71**, 095007 (2005).
9. E. A. Baltz and P. Gondolo, *JHEP* **10**, 052, (2004).
10. R. Bernabei *et al.*, *Phys. Lett.* **B389**, 757, (1996).
11. R. Gaitskell and V. Mandic, <http://dmttools.brown.edu>.
12. D. S. Akerib *et al.*, (CDMS Collab.) *Phys. Rev. D* **68**, 082002 (2003).
13. D. S. Akerib *et al.*, (CDMS Collab.) *Phys. Rev. Lett.* **93**, 211301 (2004).
14. D. S. Akerib *et al.*, (CDMS Collab.), submitted to PRD. arXiv:astro-ph/0507190.
15. D. S. Akerib *et al.*, (CDMS Collab.), submitted to PRL. arXiv:astro-ph/0509259.
16. R. W. Schnee *et al.*, (SuperCDMS Collab.), astro-ph/0502435; P. L. Brink *et al.*, (SuperCDMS Collab.), astro-ph/0503583.